The influence of saturation on the cracking process in compacted desiccating clays

Maria Noack[1,a], Paul Winkler[1] and Karl Josef Witt[1]

[1]*Bauhaus-Universität Weimar, Faculty of Civil Engineering, Chair of Geotechnical Engineering, 99423 Weimar, Germany*

Abstract. Tensile failure in unsaturated cohesive soils during desiccation is important for the design of geotechnical applications such as capping systems of landfills and sealing material of dikes. This study presents the results of different initial parameters of compacted clay samples such as gravimetric water content, dry density and degree of saturation. These parameters are varied systematically for each test to find the correlation between those parameters and the tensile failure. The tensile failure for all tests occurred by a comparable constant change of the degree of saturation. The soil specific saturation ratio $S_{r,s}$ is defined as the quotient of saturation changes ΔS_r to initial saturation $S_{r,0}$. This parameter related to the total suction shows an equal course for all results. All in all, the course of the soil specific saturation ratio $S_{r,s}$ is independent of all initial parameters. These results provide a physical and hydraulic-mechanical description for modelling the desiccation process. To demonstrate the initiation and progress of tensile failure, the experimental results are modelled with a Discrete Element Method (DEM) approach.

1 Introduction

In desiccation processes of cohesive soils due to evaporation or transfer of heat the loss of the fluid phase leads to an increase of suction in the soil which is accompanied by a noticeable change of volume. The soil shrinks. A number of researchers studied in decades this shrinkage behaviour with different focuses.

Methods of desiccation tests of clays can be divided in free (without development of cracks) and restrained (exceeding of tensile soil strength leads to cracks) shrinkage test. Most tensile strength experiments are induced by external loading and not by the internal desiccation stresses [1] or fail to incorporate stage-wise drying of soils [2], which is essential for investigations related to cracking characteristics in clays. Commonly studies investigate full saturated conditions, few researchers performed experiments on initially unsaturated and compacted clays.

This paper investigates the influence of different initial compaction parameters on shrinkage process of clays, in particular the significance of the degree of saturation. The tests were systematically conducted with samples compacted on the dry and wet side of the optimum of the standard proctor curve (σ_c = 600 kPa). To study the hydraulic-mechanically coupled correlations suction tests, free shrinkage tests, shrinkage tensile tests and restrained shrinkage tests were performed. The purpose of the test program is to provide a variety of parameters which can be put in correlation to crack initial state. In addition the cracking behaviour is modelled with Discrete Element Method (DEM).

2 Soil properties and preparation

In the test program a clay called "Plessa" was used, which is classified as a high plasticity clay with a liquid limit of w_l = *54.5%,* a plastic limit of w_p = *21.0*% and a saturated shrinkage limit at w_s = *16.7*%. The specific gravity is ρ_s = *2.691 g/cm³*. The amount of clay size particles (< *2 μm)* is *42.8%* and *57.2%* of the particles are between *2 μm* and *2mm*. The main minerals are kaolin with *18.0%* and illite with *9.0%*.

The preparation of the soil affects strongly the compaction properties of the material. To ensure reproducible and comparable test results, the clay was homogenized in accordance to the advice of Birle et al. [3]. Additionally the clay with the required water content was pushed through a sieve of *4mm* mesh size for a consistent initial sample structure.

To choose the initial conditions of dry density, water content and saturation for the experimental program three moisture-density compaction curves associated with compaction vertical stresses σ_c = 210, 400 and 600 kpa have been carried out. The results are shown in Figure 1, where contours of equal degrees of saturation are indicated.

Test point D1 is located at the dry side of the Proctor Optimum, while the test points A2, B1, B2 and B3 represent the properties at the wet side. The test points D1 (w = *17.0*%, ρ_d = *1.512 g/cm³*), B2 (w = *21.0*%, ρ_d = *1.512 g/cm³*) and A2 (w = *25.0*%, ρ_d = *1.512 g/cm³*) have different initial water contents but the same dry density. Same initial water content with different dry density have the points B1 (w = *21.0*%, ρ_d = *1.615 g/cm³*), B2 (w =

[a] Corresponding author: maria.noack@uni-weimar.de

21.0%, ρ_d = 1.512 g/cm³) and B3 (*w = 21.0%, ρ_d = 1.345 g/cm³*). Moreover the points B1 (S_r *= 84.8%*) and A2 (S_r *= 86.3%*) have a comparable initial saturation.

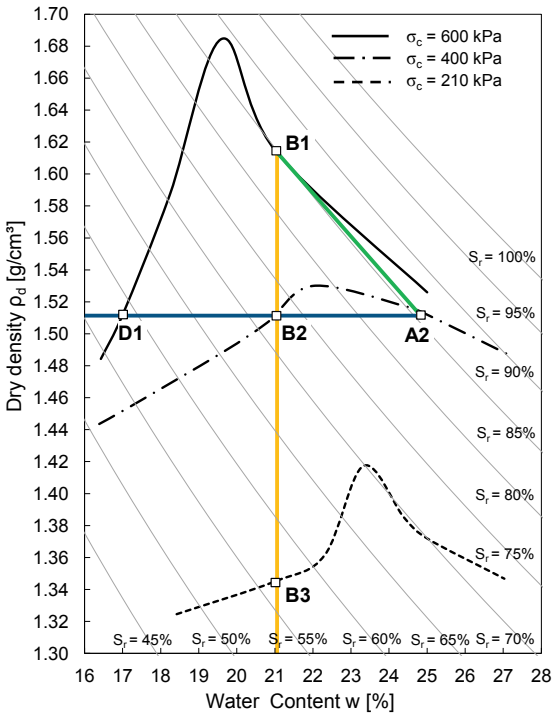

Figure 1. Static compaction curves for the vertical stresses σ_c = 210, 400 and 600 kPa

3 Setup and experimental procedure

3.1 Free Shrinkage Tests

For each of the five different compacted mounted state three samples were prepared with a diameter of *d = 7.15 cm* and a height of *h = 2.00 cm*. The samples dried without previous saturation in constant environmental conditions. During the desiccation process the changes of volume and mass were regularly measured. At the end of the experiments the samples were dried in oven and the dry densities were determined by the wax displacement method. From these experiments the changes of the volume, the dry density, the void ratio and the saturation in desiccation process are derived.

3.2 Suction Measurements

The relation between the total soil suction and the changes in water content, while the desiccation, were experimentally determined by the use of a chilled-mirror dew-point hygrometer (WP4-T by Decagon). To determine the total suction, this equipment uses the thermodynamic relation between the total suction, the relative humidity and the temperature according to the Kelvin's equation.

From large prepared free shrinkage samples three discs with a diameter of *d =3.88 cm* and a thickness of *h = 0.50 cm* has been cut. The suction measurements were performed on these discs. After each measurement the samples were weighted and air-dried to the next water content. After a homogenisation of 24 h in an airtight chamber the measurements were continued. At the end the water content was determined by oven drying. As a result besides the suction-water content-relation the pore size distribution was analyzed. The volumetric water content and the degree of saturation were determined with the dry densities of the free shrinkage tests.

3.3 Shrinkage Tensile Tests (STT)

To investigate the effect of desiccation process on the initiation and propagation of tensile cracks for each initial condition a minimum of 3 shrinkage tensile tests were performed. An illustration of the experimental setup is shown in Figure 2. The soil samples were compacted in a mould shaped like the number eight but with similar dimensioned loops. The dimension of the samples were *l = 7.21 cm* in length and *h = 1.00 cm* in height. Each end of the soil sample was covered with steel claws. While at one claw the tensile stresses during the test were simultaneously recorded by a load cell, the other claw was fixed. During shrinking process the change in water content was measured continuously. At the moment of crack initiation the dry density was determined by the wax displacement method. The purpose of these experiments was the determination of the water content, dry density, void ratio and saturation at failure state. Furthermore the duration of time until failure was determined.

It should be noted that the tensile stress measured in this setup is strongly influenced by other physical parameters like friction or transverse forces. So the measurement of the tensile stress is qualitative in character and useful to find the peak of the stress and a definition of failure.

Further investigations with an improved and advanced Shrinkage Tensile Test apparatus will be conducted.

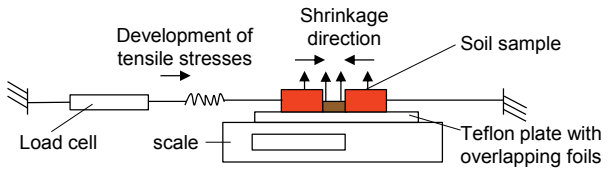

Figure 2. Shrinkage Tensile Test (STT).

3.4 Restrained Ring Tests (RRT)

An image of the setup is presented in Figure 3. At the beginning of the experiment an area of 20 cm x 35 cm of soil was compacted to the required initial parameters with a purpose-built compaction plate. The sample height was set to *h = 1.00 cm*. After the compaction two samples with an outer diameter of d_o *= 15.02 cm* and an inner diameter of d_i *= 7.62 cm* were cut out with steel rings. The remaining soil was used to determine the initial parameters of water content, dry density, void ratio and saturation. Both samples each in two steel rings were put on a Teflon foil to reduce friction at the bottom. One setup was placed on an electronic balance with an

accuracy of *0.01 g* and a recording interval of 5 values per minute. Each five minutes a high resolution digital camera (Canon PowerShot SX50 HS) recorded the changes of area in desiccation process. To prevent disturbing influence of shadows a LED ring light was direct screwed with the lens. The second sample was placed nearby and was equipped with a height sensor at the surface to determine the settlements continuously. Around the setup there are steady environmental conditions, recorded on a climate data logger.

The shrinkage displacements were calculated by geoPIV (White et al. 2003 [4]), a Matlab based particle image velocimetry (PIV) analysis. This code has been used effectively in several geotechnical engineering researches to analyze soil deformations (e.g. [1],[5]). A contrasting stochastic pattern was sprinkled randomly on the sample. From a mesh of patches of 32 by 32 pixels with a path size of less than *2.4 mm* by *2.4 mm* (1 pixel ~ *0.075 mm*) the displacements and strains were determined by the software.

To analyze the changes in area the images were convert to binary pictures, based on threshold by Matlab image processing. Geometric parameters were evaluated by the detected pixel information, which was provided by the software code.

As results of these test series the displacement, strain, volumetric change, change in dry density, water content, void ratio, saturation over the whole shrinkage process and in particular at failure can be documented.

First findings relating to the topic are presented in this paper.

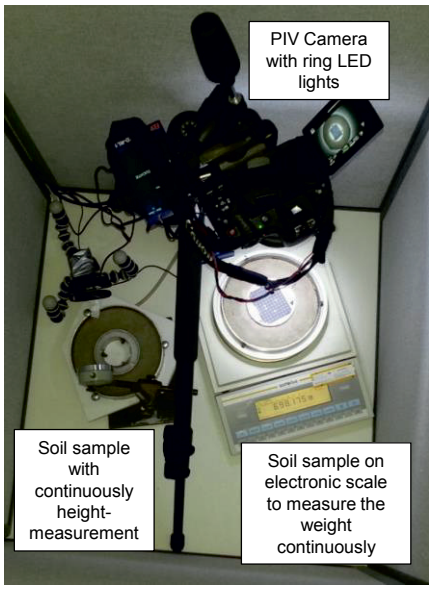

Figure 3. Restrained Ring Test (RRT) in testbox.

4 Experimental results

The total soil suction properties could be investigated in a range of *0.5-300 MPa*, which is caused in the limited determination range of the dew-point potentiometer, where capillary forces < *0.5 MPa* cannot be analysed in pores between aggregates (interaggregat pores). In Figure 4b the saturation properties over the suction data are presented. It shows the influence of different initial water contents and dry densities as well as the initial saturation. Samples with the same initial saturation (A2 and B1) show a very similar drying path independent of the different initial water content and dry density, respectively the different initial pore structures. An increase in the initial dry density at the same water content (from B3 to B2 to B1) implies on the structural properties a decrease in the bulk void ratio through the reduction of the amount of the greater pore diameters (interaggregat pores), while the amount of intraaggregat pores (pores in aggregates with smaller diameters) is continuous similar [6]. The changes in hydraulic properties are obviously in the increase of the saturation degree (from B3 to B2 to B1). These initial changes of the structural and hydraulic properties do not affect the initial suction measurements. All three samples start with equal suctions. The well known influence of increasing initial water content on same dry density (from D1 to B2 to A2) to the increase of the total suction is becoming apparent in Figure 4b.

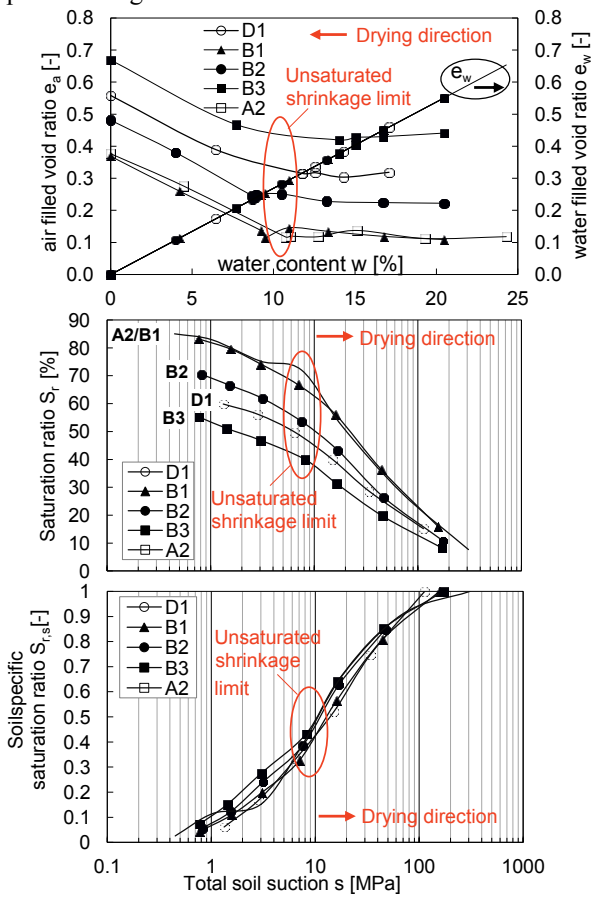

Figure 4 a, b, c. Results of free shrinkage and suction tests.

It can be seen that during the drying process the amount of changes in saturation (ΔS_r) in all samples are similar until the shrinkage limit is reached (see Figure 4b). This can be explained by the development of the air filled (left vertical axis) and water filled (right vertical axis) void ratio in Figure 4a. The water filled void ratio is the same line for all samples. Until the shrinkage limit is reached the changes of the void ratio are in accordance with the amount of changes of the water filled pores. As the relative humidity of the environmental air is for all samples similar, they dewater in the same amount,

independent of different structural properties. The amount of the air filled void ratio remains approximately constant. With occurrence of the shrinkage limit the air filled void ratio increase in the same value the water filled void ratio decrease. This behaviour is comparable identically for all samples despite several initial structural and hydraulic properties. This suggests a soil specific property over the complete desiccation process, which is graphically highlighted in the soil specific saturation ratio $S_{r,s}$ in Figure 4c:

$$S_{r,s} = \Delta S_r / S_{r,0} = (S_{r,0} - S_r) / S_{r,0} \quad (1)$$

Where S_r is the current saturation ratio and $S_{r,0}$ is the initial saturation ratio.

In the following, these properties of the compacted samples are related to the crack behaviour investigated by shrinkage tensile and restrained ring test. The determining of the parameters of these experiments has already been described (see 3.3 and 3.4). Just the development of the total soil suction has been adopted by the free shrinkage tests. In Figure 5 sample of the results of PIV analysis and the corresponding binary image in restrained ring test is illustrated.

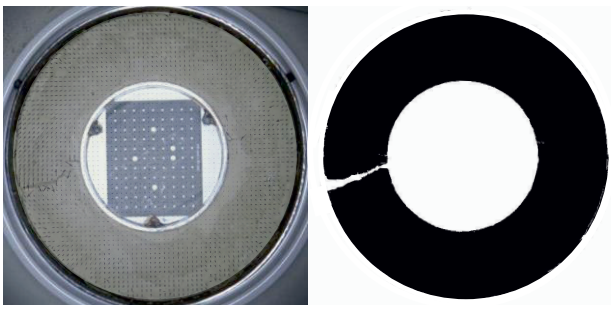

Figure 5. PIV analysis and binary image of Sample A2 complete cracked.

Table 1 highlights the most important findings subjected to the drying process and the comparison of the STT and RRT A2 results. Interesting remarks can be made about the changes of the hydraulic parameters. In particular all samples cracked approximately if the water content changed around *2-3%*. The results of STT and RRT are similar. So the occurrence of the crack appears comparable in both types of experiments.

Further conclusions can be achieved due to the addition of the results which are presented in Figure 6, where the combination of free shrinkage tests and STT results are illustrated. It is supposed that the failure state is a function of the changes in water content along the free shrinkage curve, which can be expressed in the changes of saturation. In four out of five (B1, B2, B3, A2) cases in STT series the changes of saturation from initial to failure state are between *3.69* and *4.51 %*.

The experimental determination of soil specific saturation ratio $S_{r,s}$ for the samples B1, B2, B3 and A2 is in good accordance to the measurements of free shrinkage - soil suction behaviour (Figure 4c), expressed in results of the last line in Table 1.

The reasons for divergences are the comparison of three different test series with possible fluctuations of the external impacts (differences in: human resource, compaction instruments, environmental conditions, soil properties). It should be noted that the factor time is not mentioned. Compaction conditions and crack initiation have an influence on the rate of desiccation.

Table 1. Results from initial to failure state: STT and RRT (A2)

	STT					RRT
	D1	**B1**	**B2**	**B3**	**A2**	**A2**
Δw [%]	2.84	2.17	2.36	2.10	2.89	2.74
ΔS_r [%]	5.51	4.52	3.69	3.78	3.72	3.51
$S_{r,s}$ [-]	0.093	0.052	0051	0.067	0.043	0.043
$s_{failure}$ [MPa][a]	2.861	1.107	1.072	1.065	0.731	0.731
$s_{failure}$ [MPa][b]	1.850	1.000	1.000	0.950	0.500	0.500

[a] determined by suction tests
[b] determined by diagram in Figure 4c

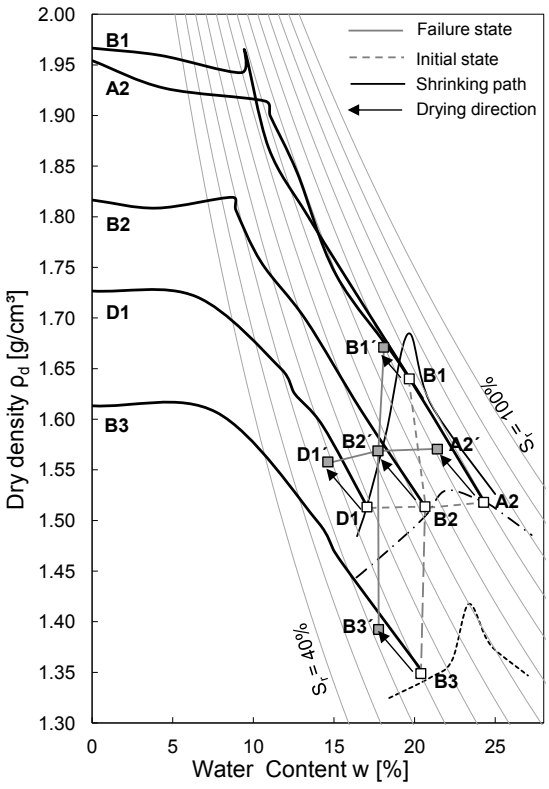

Figure 6. Results of free shrinkage test and STT.

5 Numerical simulation

The shrinking behaviour of the soil and the resulting desiccation cracks are modelled in a numerical simulation for a better understanding and the development of a theoretical model. Granular material at all and cracking in particular is not well represented in methods of continuum mechanics [7]. Therefore particle simulation with grid free methods, especially Distinct- or Discrete-Element-Method (DEM) is used.

The DEM is a numerical method, computing the motion and effect of a large number of particles [8]. It gives the opportunity to determine the discrete parameters of a particle assembly. Although DEM is related to molecular dynamics, the method is generally distinguished including rotational degrees of freedom as well as stateful contact. The application of the DEM in geomechanics was proposed by Cundall and Strack [9]. Today the DEM is well established [7] and can provide insight into the soils structure [10]. The method is computationally intensive. Several DEM codes using parallel processing to be able to simulate models with higher number of particles and longer duration. With advances in computing power and numerical algorithms for nearest neighbour sorting, it has become possible to increase the number of particles with simulations of longer duration.

Different programs (e.g. PFC3D, EDEM, LAMMPS, LIGGGHTS, Yade, WhoDEM) are available for DEM simulations. The authors use LIGGGHTS, because it is effective for high particle numbers and there is a version free of charge. LIGGGHTS is based on the molecular dynamics simulator LAMMPS and extended to support granular media [11]. The model for the simulation is described in a scripting language, which allows easy modifications of the model. The program is open source, the code can be modified and extended for individual users' needs. It is possible to import complex geometry from computer aided design (CAD) into the simulation. For further investigations a coupling with the CFD solver OpenFOAM is available [12].

The biggest disadvantage of the DEM is its computational effort for high particle numbers. Since clay consists of very small particles it is neither a granular material nor is the number of clay particles in a range which could be handled by current simulation hardware in a reasonable time. Microscopic observations show that the clay particles clump together in aggregates of various scales like a fractal structure [13]. The swelling and shrinking of clay can be explained as a behaviour of the aggregates [14]. The small clay particles gathered to this much bigger aggregates makes it possible to modell the shrinking and swelling of clay with the DEM in a numerical simulation [15], [16]. To obtain reliable results in a reasonable time, the particle size of the aggregates is varied over a range of 1 to 4 mm. This decreases the necessary particle number from 190,000 to 3,000 and results in a 60 times faster computation for testing purpose.

The Simulation consists of three steps, 1. Particle Insertion, 2. Compaction of the Sample, 3. Desiccation. In the first step a flat ring shaped bin with the measure-

Table 2. Parameters for Numerical Simulation.

Parameter	Value	Unit
Contact Model	Hertz	-
Boundaries	Periodic	-
Simulation Domain	0.1 × 0.1 × 0.1	m
Gravity	9.81	m/s²
Time Step Length	10E-7	s
Particle Size	0.001 – 0.004	m
Particle Density	2500	kg/m³
Skin depth	0.02	m
Volume Fraction Insert	0.2	-
Young's Modulus	50	GPa
Poisson's Ratio	0.35	-
Coef. of Restitution	0.3	-
Coef. of Friction	0.1	-
Coef. of Rolling Friction	0.5	-
Cohesion Energy Density	1E8	J/m³

Figure 7. With the RSA inserted particles.

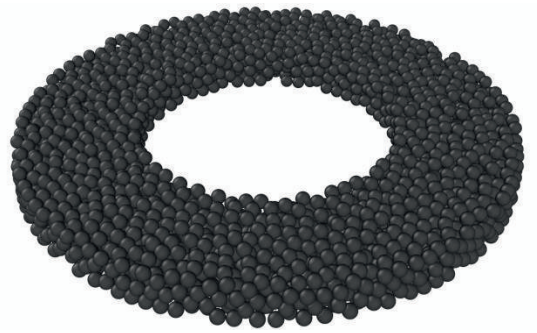

Figure 8. Compacted sample.

Figure 9. Sample with desiccation crack

ments of the sample volume is created and the simulation parameters are set up with the values given in Table 2. The clay aggregates are inserted (Figure 7) as spherical particles with the Random-Sequential-Addition-Algorithm (RSA) [17]. In this algorithm, particles are sequentially placed in the bin by random. If they overlap with existing particles they will be discarded, else they were kept. The resulted packing has a low density. In step two the particles settle by a gravitational field. For a higher packing density and an even surface of the sample a compaction plate was lowered on top of the particles (Figure 8). The test sample is now prepared like the one in the laboratory test. The porosity is about 36%, what is typically observed for random close packings of monodisperse spheres [18]. It is less than the porosity of the clay samples which is caused by the more chaotic order of the clay particles (edge-to-face flocculated fabric) [19] compared to the assembly of the isotropic shaped spheres. In the third step the desiccation of the clay is represented by the shrinkage of the clay aggregates. The loss of the volume of the water due to desiccation correlates with the decrease of the particle diameter. Whilst the particles are shrinking they stick together by the force of cohesion. The cohesion is modelled with the Simplified-Johnson-Kendall-Roberts model (SJKR) using an additional normal force contribution. Two particles in contact will have an additional normal force maintaining the contact which writes:

$$F_n = k\,A \tag{2}$$

where A is the particle contact area and k is the cohesion energy density (Table 2). Therefore during the desiccation process the particles move closer to each other. Where this particle rearrangement is restricted due to geometric boundaries or by the particles itself, restrained shrinking will occur. The force of cohesion will cause tensile stresses. Since the fabric of the particles is not regular like in a crystal, but stochastic heterogeneous, the distance, and therefore the forces, between the particles variegate. So locally particles lose contact and if the assembly is not able to cope with the rising tensile stresses in some area an incipient crack will start and propagate whilst desiccation, a crack appears (Figure 9).

6 Conclusions

A study of desiccation cracking in compacted clay based on experimental and numerical determination is presented. It is found that the failure state for all tests occurred by a comparable change of the saturation ratio ΔS_r. The soil specific saturation ratio $S_{r,s}$ presents the ΔS_r in proportion to the initial adjusted saturation ratio $S_{r,0}$. Independent of the investigated initial properties $S_{r,s}$ follows the same path in correlation to the total suction. The DEM simulation offers the suitable possibility for the grid free numerical modelling of desiccation induced cracks. Further extensive experimental and numerical research in this field will be performed.

References

1. B. Shannon, J. Kodikara, P. Rajeev, Geotechnical Testing Journal 38, 1, 98-112, (2015)
2. K. V. Uday, P. N. V. Jayanthi, D. N. Singh, Drying Technology, 32: 869-876, (2014)
3. E. Birle, D. Heyer, N. Vogt, Acta Geotechnica, 3: 191-200, (2008)
4. D. J. White, W. A. Take, M. Bolton, Geotechnique, 53, 7: 619-631, (2003)
5. N. I. Thusyanthan, W. A. Take, S. P. G. Madabhushi, M. D. Bolton, Geotechnique, 57, 6: 581-594, (2007)
6. E. Birle, Geohydraulische Eigenschaften verdichteter Tone unter besonderer Berücksichtigung des ungesättigten Zustandes. Doctoral Thesis, München, (2011)
7. C. O'Sullivan, Particulate discrete element modelling, Hoboken, NJ: Taylor & Francis, (2011)
8. P. A. Cundall, A computer model for simulating progressive large scale movements in blocky rock systems. Proceedings of the Symposium of the International Society of Rock Mechanics, Nancy. (1971)
9. P. A. Cundall, O. D. L. Strack O.D.L., Géotechnique, 29, 47 –65, (1979)
10. P. Winkler, M. R. Sadaghiani, H. Jentsch, K. J. Witt, Granular packing generation using DEM–Modified Force-Biased-Algorithm. Proc. 7th Int. Conf. on Scour and Erosion, Perth, Australia, 2-4 (p. 345). CRC Press, (2014)
11. C. Kloß, C. Goniva C., LIGGGHTS an Open Source Discrete Element Simulations of Granular Materials based on LAMMPS, Proc. TMS Annual Meeting, San Diego., (2011)
12. C. Goniva, C. Kloß, A. Hager, S. Pirker S., An Open Source CFD-DEM Perspective, Proc. of OpenFOAM Workshop, Series OpenFOAM Workshop, (2010)
13. V. Ferber, J. C. Auriol, Y. Cui, Can. Geotechnical Journal, 45, 252-65, (2008)
14. E. E. Alonso, J. Vaunat, A. Gens, Eng Geol, 54, 173-83, (1999)
15. J. Sima, M. Jiang, C. Zhou, Computers and Geotechnics, 56, 168–180, (2014)
16. A. Amarasiri, J. Kodikara, S. Costa, Int. J. Numerical and Analytical Methods in Geomechanics, DOI: 10.1002/nag.894., (2010)
17. R. Jullian, A. Pavlovitch, P. Meakin P., J. Phys. A: Math. Gen., 25, 4103–4113, (1992)
18. J. D. Bernal, Nature 183, 141 – 147, (1959)
19. J. K. Mitchell; K. Soga, Fundamentals of soil behaviour, Hoboken, NJ : Wiley, (2005)